International Journal of Geosciences, 2026, 17(11), 883-897
https://www.scirp.org/journal/ijg
ISSN Online: 2156-8367
ISSN Print: 2156-8359

Morphodynamic Response of Sandy Beach Profiles in Precambrian Basement Domain in the Tidal Cycle: The Case of the Port Area of San Pedro

Saimon Aby Atsé Mathurin[1*], Egoran Blandine Akissi Married Kouassi[2], Beugré Djahouié Prisca Married Atri[2,3], Axel Koukougnon[2]

[1]Oceanological Research Center (CRO), Abidjan, Côte d'Ivoire
[2]University of San Pedro, UFR of Marine Sciences (SDM), San Pedro, Côte d'Ivoire
[3]Université Alassane Ouattara, Bouaké, Côte d'Ivoire
Email: *saimon.aby@cro.edu.ci

How to cite this paper: Mathurin, S.A.A., Kouassi, E.B.A.M., Atri, B.D.P.M. and Koukougnon, A. (2026) Morphodynamic Response of Sandy Beach Profiles in Precambrian Basement Domain in the Tidal Cycle: The Case of the Port Area of San Pedro. *International Journal of Geosciences*, **17**, 883-897.
https://doi.org/10.4236/ijg.2026.1711041

Received: August 17, 2026
Accepted: November 20, 2026
Published: November 23, 2026

Copyright © 2026 by author(s) and Scientific Research Publishing Inc.
This work is licensed under the Creative Commons Attribution International License (CC BY 4.0).
http://creativecommons.org/licenses/by/4.0/
Open Access

Abstract

The coastline of San Pedro, located in the Precambrian basement domain, is subject to a strong morphosedimentary dynamic linked to the action of the tides and the swell. In this context, understanding the variations of the foreshore is essential to better understand the morphodynamic functioning of the beaches. This study aims to analyze the morphodynamic response of the beaches of San Pedro during the tidal cycle, in order to know the main morphological variations according to the parts of the foreshore. High-resolution altimetry monitoring was carried out in the cross-shore directions. Two field campaigns were carried out, one in February 2026 in the middle of the season of low marine unrest, the other in April 2026 at the beginning of the strong sea agitation, in order to measure altitude variations and sedimentary reworkings. Observations show a clear spatial organization: the upper foreshore remains relatively stable, the mid-foreshore presents an intermediate dynamic, while the lower foreshore records the strongest altimetry variations. The ebb generally favours fattening with a maximum of deposition at low tide, while the tide is accompanied by more marked erosion with the strongest departure at high tide. In addition, the profile located in the trough of crescents better promotes coexistence erosion fattening in the tidal phases and should present the lowest sedimentary balances. Conversely, the profile on the ridge presents more of a differentiation in trends according to the phases of the tide. Thus, the approach of low tide promotes sedimentation, whilst the approach of high tide promotes erosion This distinction is all the more pronounced when the waves are par-

ticularly strong. The study thus confirms that sedimentary transfers are highly asymmetric and spatially hierarchical according to the parts of the foreshore. This study highlights a beach in the Precambrian basement domain with an average general slope varying between 6.84 and 9.95% and medium to coarse grain size subject to a high morphodynamic intensity.

Keywords

Altimetry Monitoring, Sedimentary Amplitudes, Tidal Cycle, Beach Crescent, San-Pedro, Ivory Coast

1. Introduction

The ordinary dynamics of tropical beaches are amplified by climate change, which exposes this ecosystem, its infrastructure and its surrounding populations to the effects of coastal erosion. On the world's coastlines, [1] estimates that 70% of the coastline is eroding. In Côte d'Ivoire, the work of [2] derived from that of [3] shows 33.91% of the coast in erosion. Most of the Ivorian coastal works concern the sandy coasts of the southeast and center. The west remains less documented compared to the two sectors mentioned above. Although in the Precambrian basement domain, the San-Pedro coastline is often counted as part of the highly erosive coastline of its coastline [3]. The work of [4] reports an average erosion of 2 - 5 m/year in San Pedro aggravated by the extension of the port and the inflows of the Nawa River. [5] found a seasonal alternation between an erosion phase from May to August and a fattening phase from November to February. In addition, the segment between the tombolo and the lighthouse point remains little studied. In these rare works, very few mention high-resolution altimetry monitoring coupled with the tide gauge regime. The Precambrian basement domains of the Southwest, including the San Pedro coastline, have a particular morphology due to intercalations of sandy banks limited by boulders. These sandy banks are very sensitive to erosion and require a small scale like tidal cycle diagnosis. Thus, crossshore altimetry monitoring was carried out to quantify altimetry variations and to know the morphological construction process in a tidal cycle. It is in this perspective that the present study, entitled: "Morphodynamic response of sandy beach profiles in the Precambrian basement domain in the tidal cycle: the case of the port area of San Pedro". The main objective of this work is to analyze the cross-shore altimetry variations of the beaches of the San Pedro coastline during a complete tidal cycle, in order to better understand the sedimentary dynamics. Specifically, it is a question of knowing the process of tidal morphological construction and of deducing the amplitudes of the resulting instantaneous and cumulative rearrangements.

2. Methodology

This study is based on field data collected along the tombolo-lighthouse axis (**Figure 1**). These data are those of continuous altimetry monitoring of submerged

foreshore in a tidal cycle.

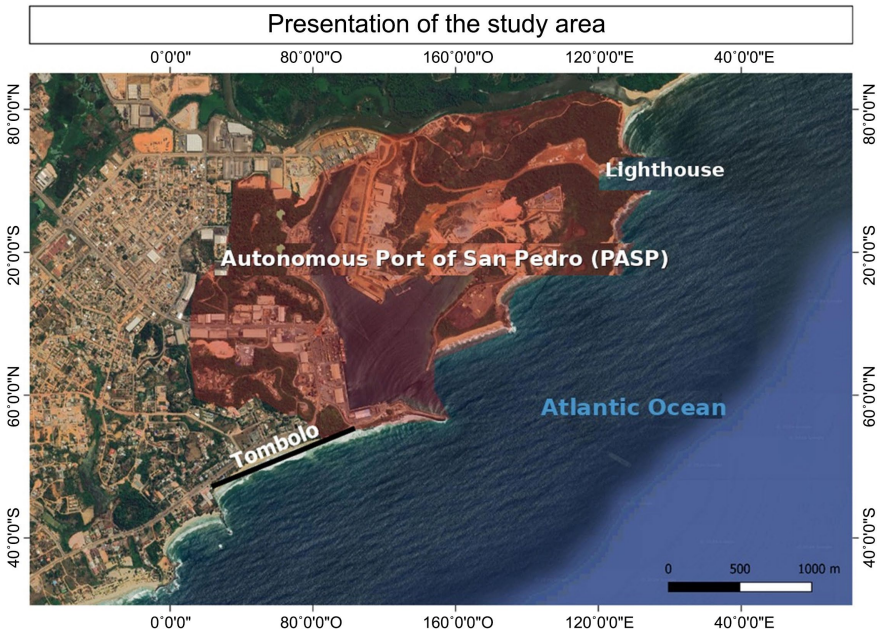


Figure 1. Presentation of the study area.

2.1. Altimetry Monitoring of the Foreshore

It is implemented on two cross-shore profiles 20 m apart. One, profile A is located in the hollow and the other, profile B on the crest of the crescent beach. Stakes (iron rods) are installed in the profile every 2 meters from the limit of the previous high tide mark to the lower foreshore. The monitoring consists of recording the heights of the iron rods as the waves pass every 5 minutes (**Photo 1**). Manual measurements taken using a tape measure marked in mm may be subject to an error of ±2 mm. Two field campaigns have been carried out; on February 11, 2026 under weak sea unrest and in April 2026 at the beginning of strong unrest. This classification, based on practical field observations and reflected in a 13.9-metre widening of the upper limit of the swash zone from 11 February 2026 to 17 April 2026 on Profile B, was also discussed by [6]. This author has identified April as the start of the period when swells occur frequently. The profile in the hollow is designated A and the one on the ridge west of A is designated B. Each profile has a number of points depending on the width of the foreshore discovered. Thus, for the campaign of February 11, 2026, thirteen (13) points were implemented on profile A and 8 on profile B (**Figure 2**). For the April 2026 campaign, 14 points on profile A and 12 points on profile B were implemented (**Figure 2**). The points are numbered in ascending order from the upper foreshore to the lower foreshore. For a particular campaign, points of the same number are located at approximately the same latitude. Whether a point belongs to a part of the swash zone was determined by combining the submergence ratio proposed by [7] with changes in slope. Thus, the points]1; 4] are classified as upper swash, the points]4; 10] are classified as mid-swash and the points]10; 14[are classified as lower swash.



Photo 1. Procedure for recording the altimetry monitoring of the foreshore.

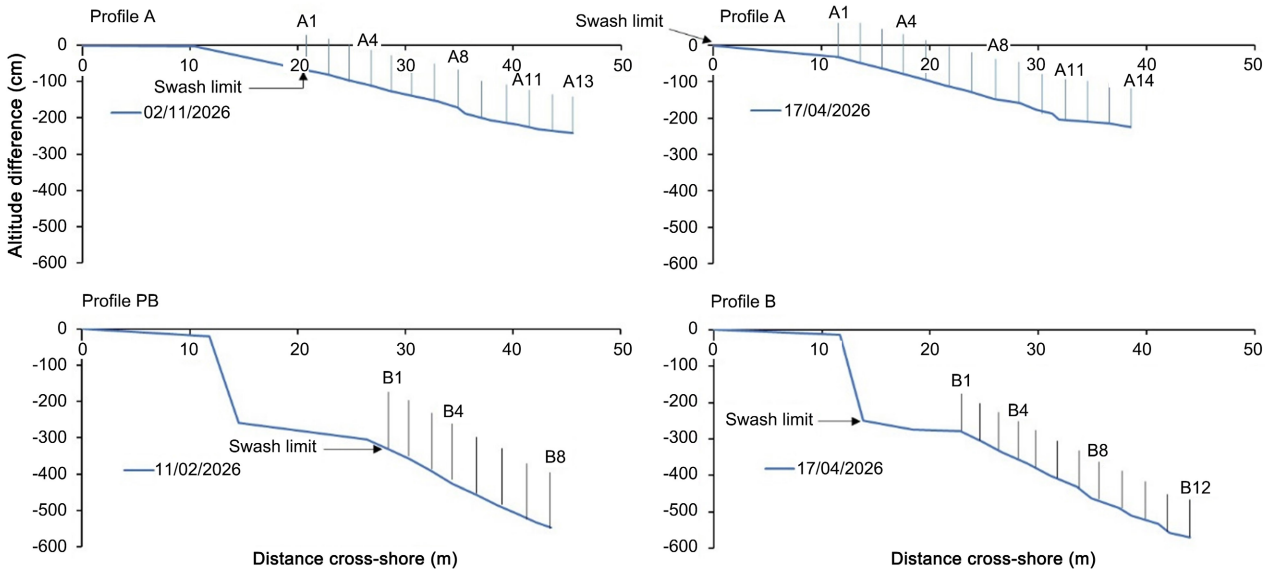


Figure 2. Layout of elevation monitoring points in the beach topographic profile.

2.2. Topographic Survey

To this monitoring is coupled a topographic survey by site level (BOSCH GOL 32 G and a 5 m foldable rod) at low water of the two altimetry monitoring profiles. The topographic survey is done in one direction from two landmarks behind the beach to the last point seaward of the elevation monitoring points.

2.3. Restitution of Altimetry Monitoring Data

The altimetry monitoring data were then processed and allowed two parameters to be deduced:

- instantaneous resulting reshuffling (IrR): This is the difference in stake heights (sh) between two consecutive dates. The measurement date is every 5 minutes. The IrR expresses the spontaneous action of waves on the sand.

$IrR = sh(t) - sh(t+1)$. A positive IrR reflects instantaneous accretion and a neg-

ative IrR reflects instantaneous erosion.

- the cumulative resulting reshuffle (CrR): this is the cumulative sum of the RrI over the duration of the follow-up. It expresses the morphology of a point on the foreshore. It is obtained by $CrR(t+1) = CrR(t) + IrR(t+1)$. A positive CrR reflects accretion and a negative CrR reflects erosion.

2.4. Restitution of Topographic Survey Data

A mathematical calculation system is applied to each survey according to its operating mode on the Excel spreadsheet.

2.5. Restitution of Tide Gauge Data

The data of the theoretical tide gauge are derived from the data of the water levels of the shom on behalf of the Port of San-Pedro on the days of the altimetry monitoring. Thus, the average daily tidal range is 0.25 m on 11/02/ 2026 and 1.04 m on 17/04/2026.

3. Results and Discussion

3.1. Cross-Shore Morphological Itinerary of the Beach Profile Points

3.1.1. Altimetry Monitoring of the Low Agitation of 11 February 2026

All the points (A1 - A12, B1 - B8) show variable morphodynamic behaviours depending on their positions on the foreshore during the tidal cycle.

✓ During the flow (07:35-13:53)

- Bottom point swash]A10; A12[: Profil B, with an overall average slope of 9.95%, has a baïne at the bottom of the beach that does not offer the possibility of being followed. Profil A, with an overall average slope of 6.84%, offers the possibility of being followed in this part of the beach. The amplitudes of the RrI values are between −6.7 cm (A11, A12) and 7.7 cm (A12). These values induce fattening with values between −3.5 cm (A12) and 8.8 cm (A12) (**Figure 3**).

- Points of the mid-wash]A4; A10],]B4; B8]: The amplitudes of the RrI on the profil A are between −10.5 cm (A10, A9) and 9.5 cm (A10). On profil B, they vary between −9.4 cm (B6) and 10.9 cm (B6). The values of the RrI are more or less the same on the crest as in the trough. The resulting morphologies of the RrI are a fattening at A10 whose surface decreases towards the high foreshore to reach an equilibrium at A9, then a trend reversal which gives an erosion from A8. The values of the RrC vary between −10.5 cm (A9) and 8.1 cm (A10). All the points of the profil B have been fattened at altitudes between −6.9 cm (B7) and 12.7 cm (B5) (**Figure 4**).

- Upper swash points]A1; A4],]B1; B4]: The effects of the previous low tide are felt by the near absence of waves. Those that have been able to do so over the duration of the flow, give altimetry levels between −6.6 cm (A3) and 6.6 cm (A3). The morphologies are invariant or stable or begin to erode on profile A on the ridge or fattening on profile B in the hollow (**Figure 4**). The altimetry variations

are between −4 cm (A4) and 5.5 cm (A3) on profile B and between −4.8 cm (B3) and 6.1 cm (B3).

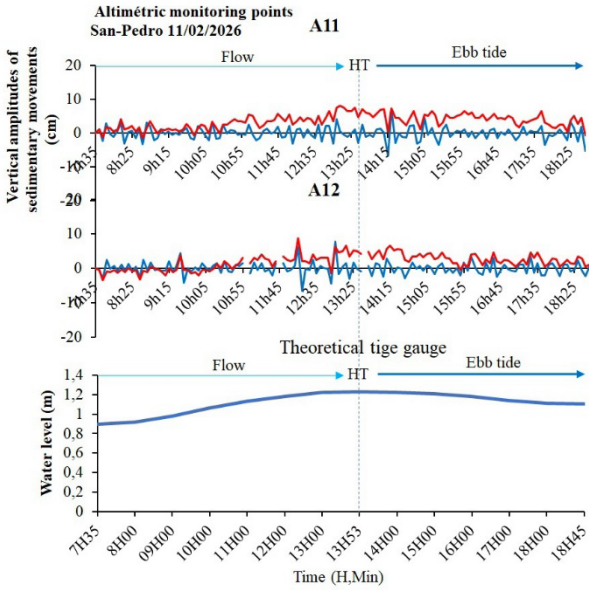


Figure 3. Morphological evolution of the lower swash points of profile A of San Pedro beach during the tidal cycle of 11/02/2026.

✓ During the ebb (13:53-18:45 min)

- Bottom point swash]A10; A13[: The amplitudes of the RrI are between −5.2 cm (A11) and 3.5 cm (A12). These amplitudes communicate a fattened morphology. The smallest altimetry level compared to the initial level reflected by the RrC curves is −0.7 cm (A11) and the largest is 5.5 cm (A11) (**Figure 4**).

- Mid-swash points]A4; A10],]B4; B8]: The amplitudes of the RrI vary between −8.7 cm (A10) and 7 cm (A6). These amplitudes vary between −5 cm (B8) and 5 cm (B5). These values reveal a stronger wave dynamic on the crest than in the trough. The fattened morphologies in the lower range continue on points A10 and A9 but with decreasing fattened surfaces so that points A8 and A7 present an almost equilibrium in comparison with their initial altimetry levels. From A6 onwards, the erosive trend appears and continues in A5. The altimetry levels resulting from wave action are between −6.2 cm (A6) and 6.5 cm (A10) on profile A. These values range from −3.6 cm (B7) to 10.1 cm (B6). The morphology at each point of the B profile is a fattening (**Figure 4**).

- Stitches at the top swash]A1; A4],]B1; B4]: The effects of the high tide are felt at these points. They are indeed submerged even though they were not in the flood phase. The amplitudes of the RrI range from −6.6/+6.6 cm (A3) to −8/+8.8 cm (B4). The amplitudes are stronger on the profile B on the ridge. The morphology in the ebb phase is very controversial. Each profile expresses its own morphology. On profile A in the hollow of the crescent, all the points erode except for point (A2) which undergoes a slight fattening. Altimetry levels; compared to the initial points, vary between −2.8 cm (A4) on the eroded points and 0.2 cm (A2) on the

fattened point. Whereas on profile B on the crest of the crescent, the points become fatter or alternate between fattening and erosion (Figure 4). The altimetry variations are between −3.8 cm (B3) and 7.9 cm (B4).

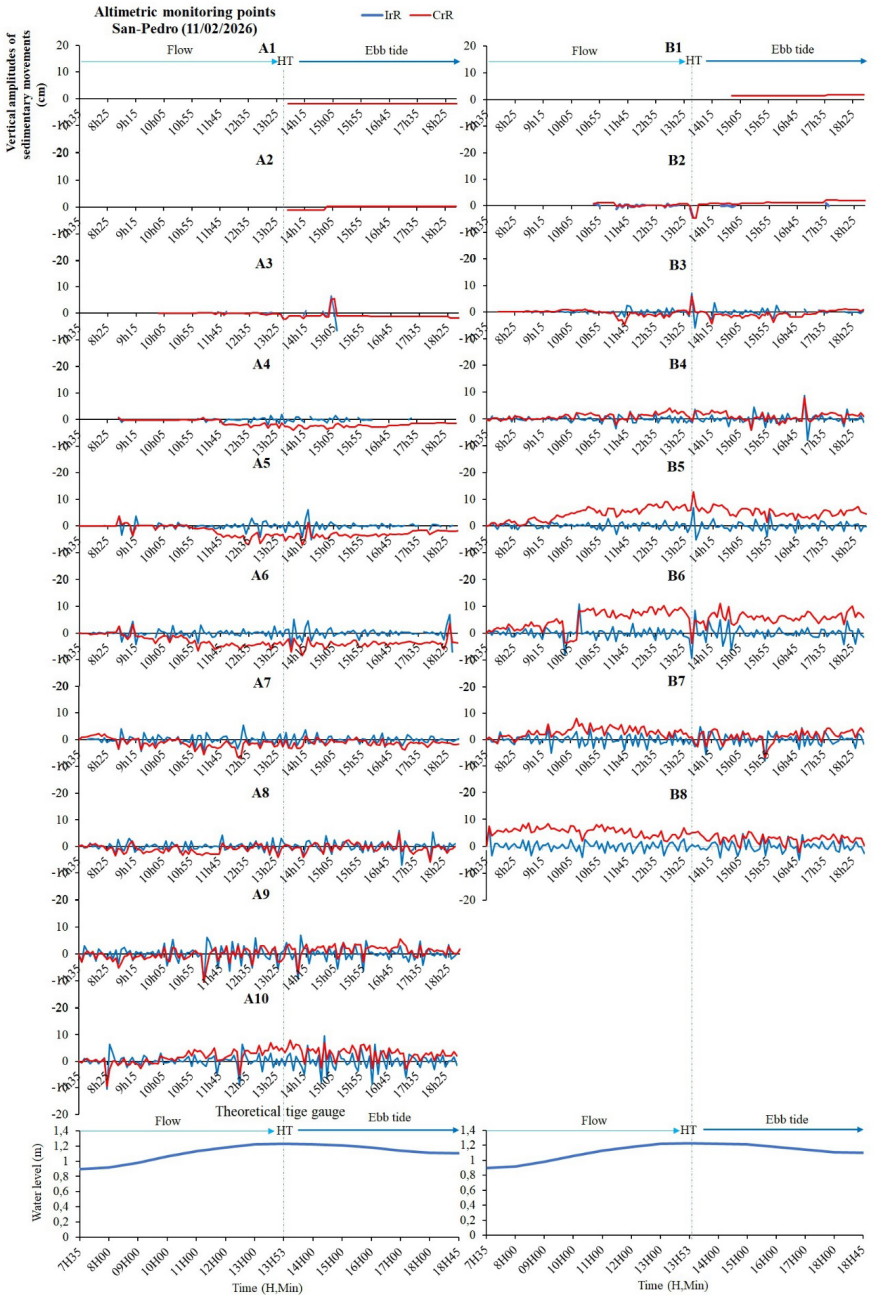


Figure 4. Morphological evolution of the upper and mid-swash points of profiles A and B of San Pedro beach during the tidal cycle of 11/02/2026.

3.1.2. Altimeter Monitoring of the Low Agitation of April 17, 2026

The altimetry monitoring of 17/04/2026 is part of two ebb phases: the first at the beginning of the monitoring from 06:55 to 10:29 at low tide (BM) and the second of high tide at 16:42 to 18:10 at the end of the monitoring. The flow phase extends from 10:29 a.m. to 4:42 p.m. The average tidal range over the duration of the mon-

itoring of 1.13 m compared to 0.25 m on 11/02/2026 causes high water levels and a retreat of 12.9 m of the swash area on profile B on the ridge and more than 20 m on profile A in the hollow of the crescent beach. This retreat of the swash area has led to a redistribution of monitoring points in the beach profile.

✓ During the ebb and tide

- Mid-wash points]A8; A14[and]B8; B12[: The high water levels engulfed the monitoring stakes and did not favour their permanent monitoring. The heights of the sand reworked during the monitoring times are between −10 cm (A9) and 10 cm (A10) on profile A and between −6 cm (B9, B10) and 6 cm (B11). These values induce a fattened morphology with larger accumulated surfaces on the B profile on the ridge than on the A profile (Figure 5). The resulting thicknesses of these altimetry levels are between −1 cm (A10) and 19.8 cm (A11) on profile A and between −7 cm (B12) and 26.8 cm (B9) on profile B.

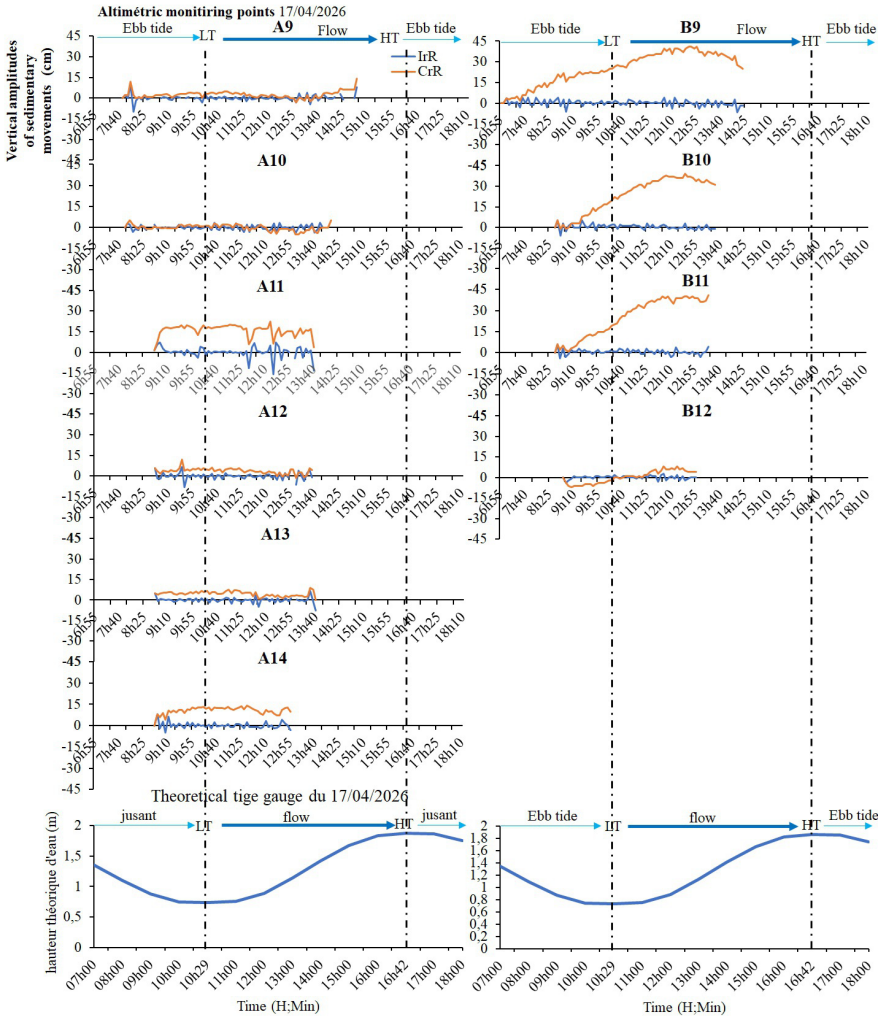


Figure 5. Morphological evolution of the mid-wash points of profiles A and B of San Pedro beach during the tidal cycle of 17/04/2026.

- Upper swash points:]A1; A8] and]B1; B8]: The vertical amplitudes of the sand movements are between −11 cm (A6) and 15 cm (A6) on profile A. On pro-

file B, these amplitudes vary between −7 cm (B5) and 8 cm (B6). Conversely, at the February follow-up, the amplitudes are greater on the A profile in the trough. The altimetry values of the RrC range from −21.5 cm (B5) to 19.7 cm (B8). These values range from −12 cm (A7) to 20 cm (A7). One could say that the long shore morphological construction mechanism is made up of sediment input on the ridges while the hollows are emptied of their sedimentary content. When a certain threshold is reached, the trend is reversed. The hollows are filled into the detriment of the ridges which are emptying. Thus, profiles A and B show two opposite trends. Profile A is getting fatter and profile B is eroding (Figure 6).

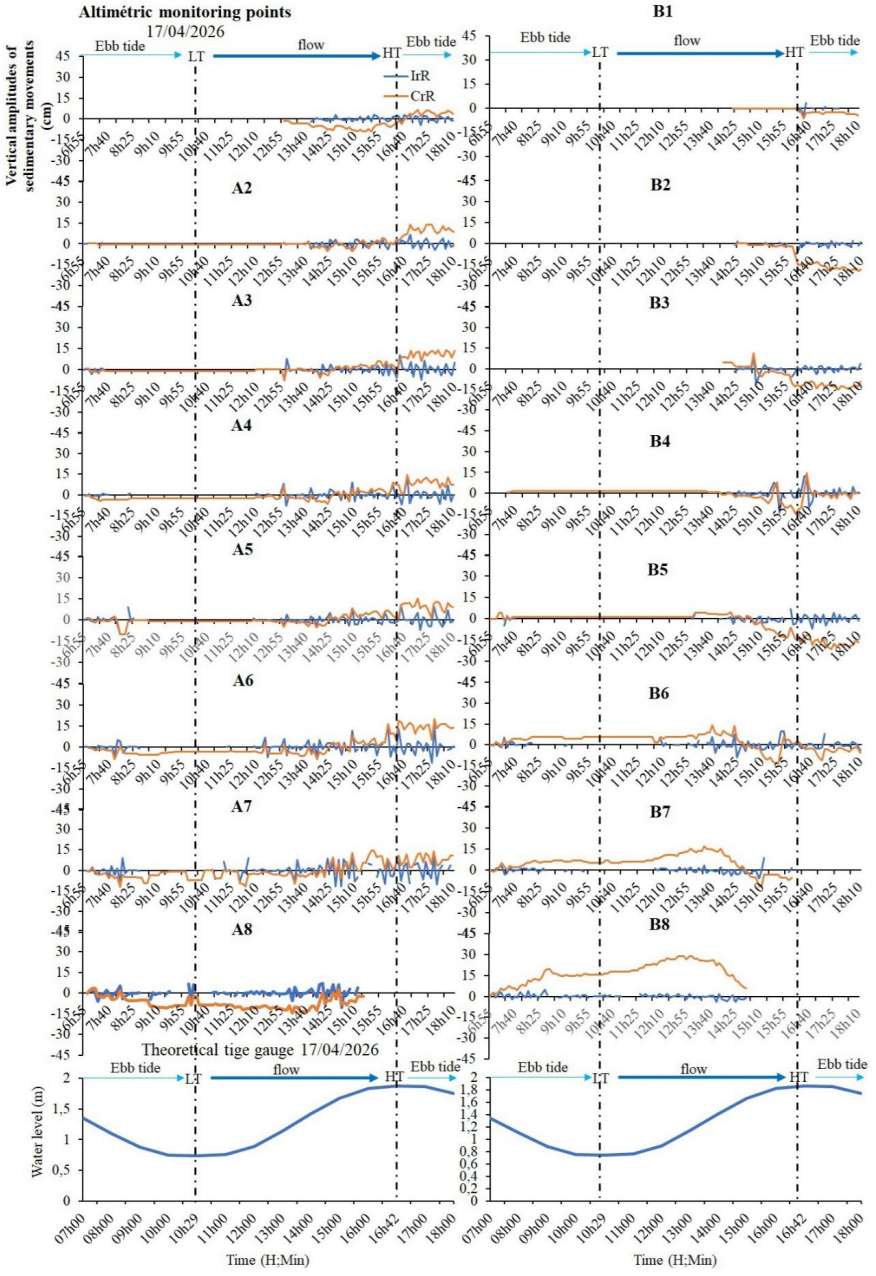


Figure 6. Morphological evolution of the upper swash points of profiles A and B of San Pedro beach during the tidal cycle of 17/04/2026.

✓ During the flow

- Points of the mid-wash]A8; A14[and]B8; B12[

The spontaneous action of the waves can tear up to −16 cm (A11) and bring up to 8 cm (A10) of sand in the 5-minute interval on profile A. These values on the B profile become −6.5 cm (B9) and 4.5 cm (B10). All morphologies have gained weight in this phase with the maximum amount of fattening on profile B. Thus, the values accumulated over the duration of the monitoring of the spontaneous wave action are between −5 cm (A10) and 22.5 cm (A11) on profile A and between −2 cm (B9) and 41.1 cm (B11) on profile B (**Figure 5**).

- Upper swash points]A1; A8] and]B1; B8]

The variations in the altimetry levels of the foreshore by wave action are between −14.5 cm (A8) and 13 cm (A6) on profile A. These values become −14.2 cm (B4) and 12.9 cm (B4) on the B profile. The cumulative duration of the monitoring of the spontaneous wave action generates amplitudes between −14.5 cm (A8) and 18.5 cm (A6) on the A profile. On profile B, these values become −16.5 cm (B5) and 28.7 cm (B8). In this part, the ridge and trough zones do not have the same morphological responses to the same hydrodynamic factors. All the points erode on profile A in the hollow, while those on profile B on the ridge become fatter. In general, during the duration of monitoring as it approaches the open tide, there is a swelling in the hollow and erosion on the ridge. On the other hand, as low tide approaches, erosion in the hollow and fattening on the ridge (**Figure 6**).

3.2. Morphological Evolution of the Profile at Different Stages in the Tidal Cycle

3.2.1. Tidal Cycle of 11 February 2026

Profile A (PA) located in the crescent hollow of the beach, shows a behavior similar to profile B (PB) on the ridge but with important morphological nuances. Six states in the cycle were studied. At 08:00, which corresponds to 25 minutes after the start of the monitoring and which represents on the tidal scale 02:09 after low tide (BM+02:09) in the tide phase, we can see that both profiles are getting fatter. The fattened surface area is greater on the profile B than on the profile B (**Figure 7**). At 10:00 a.m., *i.e.* 04:09 a.m. after low tide (BM+ 09:09 a.m.), the fattened area increased on each of the profiles. There is the appearance of a more extensive eroded surface on profile A than on profile B. As it approached high tide, 01 H 53 min before high tide (PM-01 H 53min), the eroded surface still extended on profile A and disappeared on profile B, leaving only the fattening (**Figure 7**). At high tide (PM) at 13 H 53 min, the area fertilized on profile A increased. The eroded part has also extended in length. On profile B, the fattening is maintained by spreading further north. This morphological configuration made up of alternating erosion/fattening with fattening lodged further down the beach is preserved, 02 H 07 min after high tide (PM+ 02 H 07 min) and 01 H 00 before low tide (BM-01 H 00). However, these areas decrease as low tide approaches. On profile B, fattening is maintained during these periods with a decrease in the area fattened as low tide approaches. In short, profile A in the hollow of the crescent beach has alternated

erosion and fattening at the top and mid-swash with an increase in surface area as it approaches high tide and a decrease as it approaches low tide. Profile B on the crest, on the other hand, has retained only the fattening with an increase in surface area as it approaches high tide and a decrease as it approaches low tide (Figure 7). Sedimentary activity is more intense when approaching high tide than when approaching low tide.

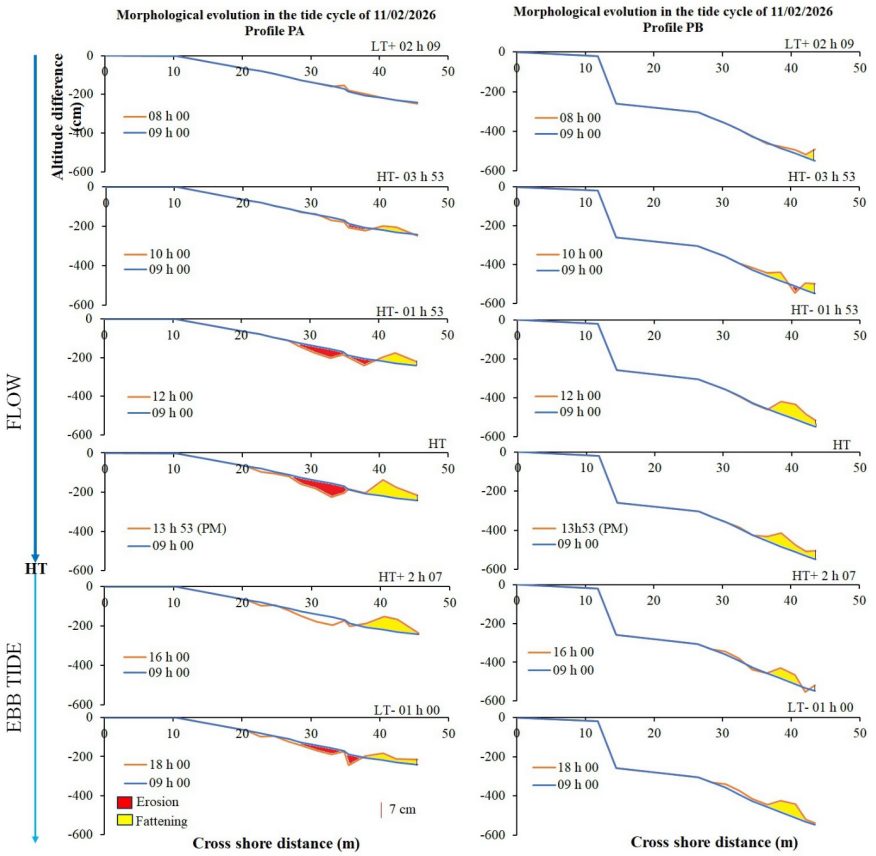


Figure 7. Morphological evolution of the submerged foreshore in the tidal cycle of 11/02/2026 on profiles A (hollow) and B (crest) of the beach crescent.

3.2.2. Tidal Cycle of April 17, 2026

Eight (8) states in the tidal cycle were analyzed. After 01 H 05 min of monitoring, which corresponds to 02 H 09 min before low tide in the tidal cycle, the two profiles A and B have fattened but with a larger surface area on profile B. 29 min before low tide (BM-29 min), at low tide (BM) and 01 H 31 min after low tide, each of the A and B profiles has adopted the same morphological behaviour: The A profile in the hollow shows both erosion at the top and mid-wash and fattening at the bottom swash. As the ebb descends, tending towards low tide, the fattened surface decreases and the eroded surface increases. Profile B, on the other hand, preserves and amplifies the fattened surface (Figure 8).

42 minutes before high tide, profound changes take place on each of the profiles. The high water levels prevent a low swash from being tracked on the A-profile in the dip. Erosion of the upper and mid-swash replaces fattening on profile

A and on profile B erosion arises for the first time in the tidal cycle.

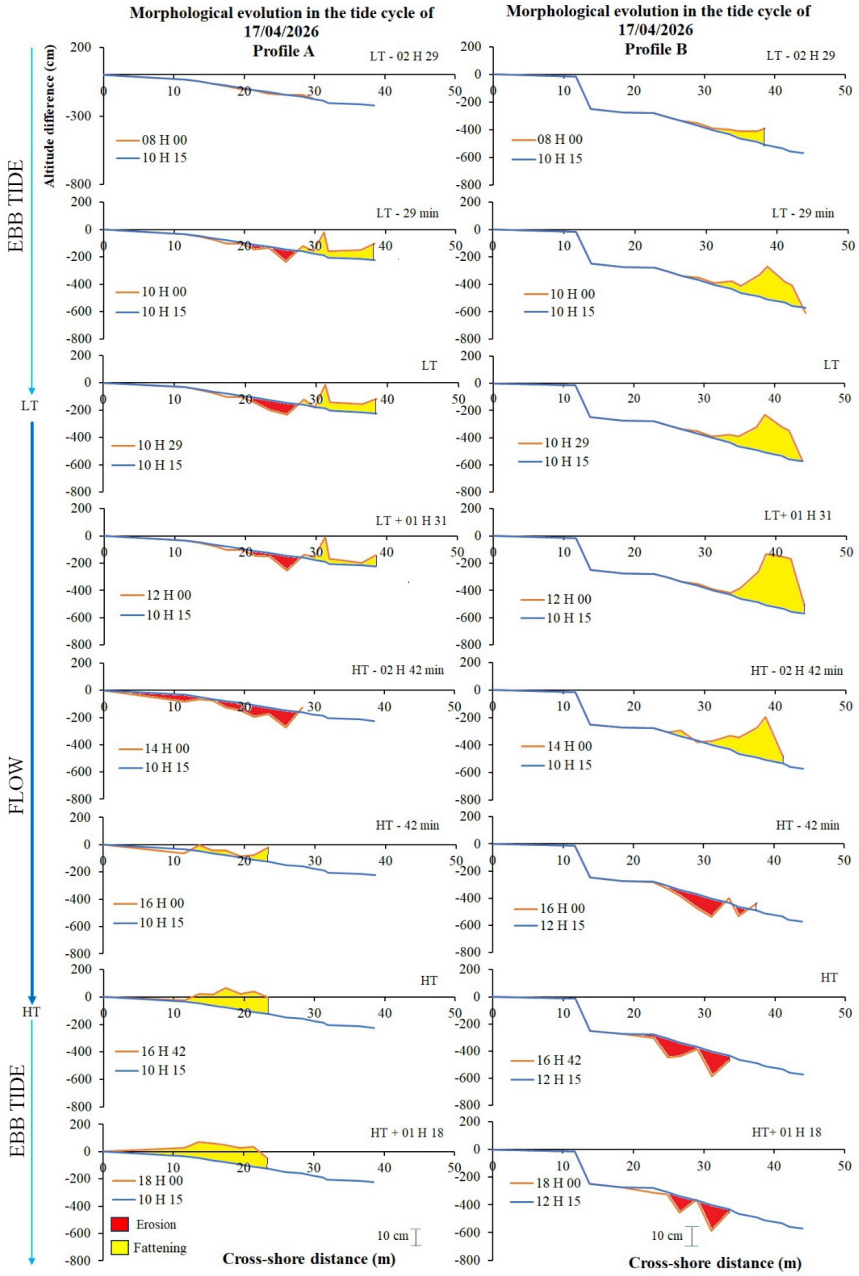


Figure 8. Morphological evolution of the submerged foreshore in the tidal cycle of 17/04/2026 on profile A in a beach crescent hollow.

At high tide (PM) and 01 H 18 min after high tide (PM+ 01 H 18 min), the two profiles retain the same morphologies. Profile A remained in fattening and Profile B remained in erosion (**Figure 8**).

Analysis in the complete cycle reveals different morphological responses depending on whether we are in the trough or on the crest. The A profile in the hollow allows erosion and fattening to coexist, with erosion at the top and mid-swash in the ebb phase up to low tide and shortly thereafter.

A reversal of morphological trends takes place in the vicinity of the open sea and remains after the high tide. Profile A in the hollow is getting fatter and profile B on the ridge is eroding.

4. Discussion

The results obtained at San Pedro show a clearly differentiated spatial morphodynamic organization according to the position on the foreshore during the tidal cycle. In general, the upper foreshore is distinguished by low mobility, the mid-foreshore by an intermediate dynamic, and the lower foreshore by a more sustained morphosedimentary activity. This hierarchy of responses confirms that the intensity of sedimentary reshuffling increases as one descends towards the sectors most frequently affected by waves**.** On the high foreshore, the points observed remain generally stable during the ebb tide, due to their low exposure to the direct action of the waves. This relative morphological inertia reflects a low sensitivity of this area to hydrodynamic forcings at the scale of the tidal cycle. Such behaviour is consistent with the observations of [8], who emphasize that the morphodynamics of the reflective and intermediate ranges are strongly controlled by the slope and frequency of immersion. The mid-foreshore presents a more contrasted response. The variations become more noticeable as you go down the foreshore, under the effect of the gradual advance of the breaking front. Alternations between fattening and erosion are more frequent, but remain moderate. This intermediate behaviour is in line with the work of [9]**,** for whom steeply sloping beaches experience an asymmetrical distribution of sedimentary flows between tide and ebb tide, with the retreat of the sea favouring a net transport to the top of the beach. It also reflects the morphodynamic transition between a zone that is not very mobile and a zone that is more actively reshuffled. in hydrodynamic energy intensifies the erosive action of the waves and often reverses the initial trend. This pattern is consistent with the results of [10] and [11] on Ivorian beaches, which highlight rapid alternations of accretion and erosion on generally stable profiles. It also agrees with the analyses of [8], The lower foreshore is the most dynamic area of the profile. It is in this sector that the amplitudes of reworking are the greatest, with a rapid alternation between accumulation and erosion phases. During the ebb tide, fattening generally dominates, as the drop in sea level favours sedimentary deposition. On the other hand, at the waves, the gradual increase according to which beach slope and wave energy directly condition the asymmetry of sedimentary transfers during the tidal cycle. The comparison between profiles A and B also shows that the morphology of the beach crescents strongly modulates this dynamic.

The profile located in the hollow of the crescent better balances cross-shore transport; by the coexistence of a surface that is fattened and eroded in the cycle. On the contrary, the profile on the ridge frequently retains a single sedimentary trend. This contrast confirms that the morphological position on the crescent controls the local redistribution of sediments, in line with the work of [12] and [13],

who showed that beach crescents generate differentiated hydrodynamic circulation cells, favoring deposition in hollows and erosion on exposed parts.

Finally, the amplitudes measured in San Pedro appear to be higher than those reported in several comparable environments. This could be attributed to the high wave energy and coarse grain size. This interpretation is consistent with the relationships established by [14] between slope, sedimentary texture and morphological mobility, as well as the observations of [15] on reflected coarse sand beaches. In this context, San Pedro is distinguished by a strong morphodynamic reactivity, where the ebb generally favours sedimentary accumulation while the flow gradually becomes more erosive.

5. Conclusion

The beaches of San Pedro have a strong morphodynamic reactivity to tidal cycles, where the ebb generally favours sedimentary accumulation while the flood intensifies erosion. The morphology of the beach crescents plays a decisive role in the local redistribution of sediments, accentuating the contrasts between hollows and ridges. The maximum amplitudes of sedimentary reshuffling vary according to the seasons: that of the weak unrest in February gives −10.5/12.7 cm. The one in April on the border of the weak and strong agitation gives −21.5/41.1 cm. These values are obtained at the mid-swash. The study provides essential elements for an integrated and preventive management of coastal zones, especially in Precambrian basement environments where morphodynamic mechanisms are still poorly documented.

Conflicts of Interest

The authors declare no conflicts of interest regarding the publication of this paper.

References

[1] Bird, E. (1993) Submerging Coasts. The Effects of a Rising Sea Level on Coastal Environments. John Wiley and Sons, 184 p.

[2] Saimon, A.A.M., Toure, M., Gbegbe, M. and Kouakou, A.M. (2026) Caractérisation des processus morpho-sédimentologiques sur un estran adossé à un trait de côte stable: cas du secteur littoral de Port-Bouët bidet (Abidjan, Côte d'Ivoire). *Revue de Géographie Tropicale et D'environnement*, No. 1, 35-49.

[3] Koffi, K.P. (2017) Contribution to the Study of the Morpho-Sedimentary Evolution of the Ivorian Coast: Sedimentary Reworking at the Multitemporal Scale. Ph.D. Thesis, University Félix Houphouët-Boigny, 322 p.

[4] Yao, K.S., Abe, J., Bamba, S.B., Konan, K.E. and Aka, K. (2010) Dynamique d'un périmètre littoral portuaire: La côte de San Pedro, sud ouest de la Côte d'Ivoire. *Revue paralia*, **3**, 2.1-2.12. https://doi.org/10.5150/revue-paralia.2010.002

[5] Abe, J. (2005) Contribution à la connaissance de la morphologie et de la dynamique sédimentaire du littoral ivoirien (cas du littoral d'Abidjan) Essais de modélisation en vue d'une gestion rationnelle. Thèse de Doctorat d'Etat es. Sc. Nat., Univ. Abidjan, 345 p. https://fr.scribd.com/document/354072437/These-D-Etat-j-ABE-2005

[6] Dangui, N.P. (2025) Effets du réchauffement climatique sur les paramètres de houle

au large de la Côte d'Ivoire entre 1985 et 2022. *DaloGéo*, No. 12, 59-68. https://www.revuegeo-univdaloa.net/sites/default/files/2025-11/DaloGéo_012_06.pdf

[7] Aagaard, T. and Hughes, M.G. (2006) Sediment Suspension and Turbulence in the Swash Zone of Dissipative Beaches. *Marine Geology*, **228**, 117-135. https://doi.org/10.1016/j.margeo.2006.01.003

[8] Masselink, G. and Short, A.D. (1993) The Effect of Tidal Range on Beach Morph Dynamics and Morphology: A Conceptual Beach Model. *Journal of Coastal Research*, **9**, 785-800. https://www.jstor.org/stable/4298129

[9] Bonnot-Courtois, C., Bassoulet, P., Tessier, B., Cayocca, F., Le Hir, P. and Baltzer, A. (2008) Remaniements sédimentaires superficiels sur l'estran occidental de la baie du Mont-Saint-Michel. *Revue européenne de génie civil*, **12**, 51-65. https://doi.org/10.3166/ejece.12.51-65

[10] Kouakou, K.A. (2025) Morphosedimentary Dynamics of Port-Bouët Beach (Abidjan, Côte d'Ivoire): Altimetry Monitoring and Sediment Balance. Master's Thesis, University Félix Houphouët-Boigny, 98 p.

[11] Saimon, A.M. (2017) Contribution of Sedimentary Reworking in the Characterization of the Mobile Layer at the Scale of the Tidal Cycle of the Coastal Sector of Abidjan. Ph.D. Thesis, University of Félix Houphouët, 238 p.

[12] Coco, G., Huntley, D.A. and O'Hare, T.J. (2000) Investigation of a Self-organization Model for Beach Cusp Formation and Development. *Journal of Geophysical Research*: *Oceans*, **105**, 21991-22002. https://doi.org/10.1029/2000jc900095

[13] Calvete, D., Dodd, N., Falqués, A. and van Leeuwen, S.M. (2005) Morphological Development of Rip Channel Systems: Normal and Near-Normal Wave Incidence. *Journal of Geophysical Research*: *Oceans*, **110**, C10006. https://doi.org/10.1029/2004jc002803

[14] Wright, L.D. and Short, A.D. (1984) Morphodynamic Variability of Surf Zones and Beaches: A Synthesis. *Marine Geology*, **56**, 93-118. https://doi.org/10.1016/0025-3227(84)90008-2

[15] Masselink, G., Austin, M., Tinker, J., O'Hare, T. and Russell, P. (2006) Cross-Shore Sediment Transport and Morphological Response on a Macrotidal Beach with Intertidal Bar Morphology, Truc Vert, France. *Marine Geology*, **251**, 141-155. https://doi.org/10.1016/j.margeo.2008.01.010